JOURNAL OF SOLID STATE CHEMISTRY

Volume 178, Number 12, December 2005

CONTENTS

Regular Articles

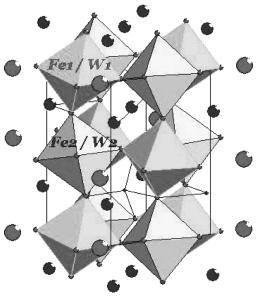

The monoclinic perovskite structure of $Ca_3Fe_2WO_9$.

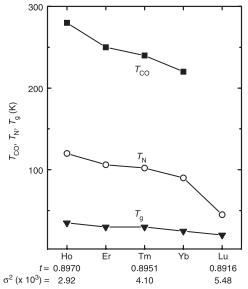

The values of T_{CO}, T_N, and T_g against the Ln ion for all the $Ln_{0.5}Ca_{0.5}MnO_3$ studied (Ln: Ho–Lu).

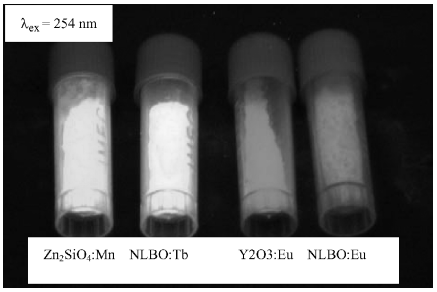

The picture of $Na_3La_2(BO_3)_3$:Ln(Ln = Tb^{3+}, Eu^{3+}) phosphors under Mercury-free fluorescence lamp.

Regular Articles—Continued

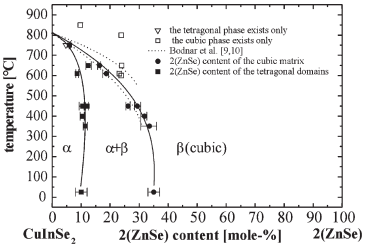

Two-phase region in the system $2(ZnSe)_x(CuInSe_2)_{1-x}$ for different temperatures (terminated by full lines). The bold squares represent the composition of the tetragonal phase and the bold circles that of the cubic one. According to Bodnar et al. (Inst. Phys. Conf. Ser. 152 (1997) 119) the two-phase coexistence area was found between both dotted lines.

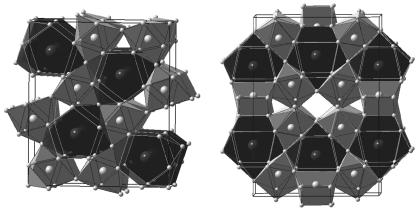

Crystal structure of $PrCo_2Al_8$ and $Pr_2Co_6Al_{19}$.

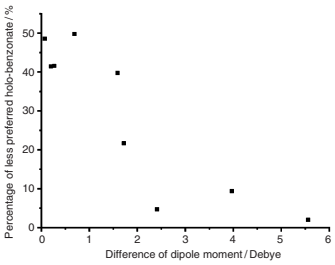

All the geometric isomers of the nine benzoate derivatives have been intercalated into $[LiAl_2(OH)_6]Cl \cdot H_2O$ in 50% (v/v) water/ethanol solution. Competitive intercalation studies using binary mixtures of the isomeric benzoates suggest that dipole moment may be a good general index for the preference.

Structural investigations of β-$CaAlF_5$ by coupling powder XRD, NMR, EPR and spectroscopic parameter calculations

M. Body, G. Silly, C. Legein, J.-Y. Buzaré, F. Calvayrac and P. Blaha

Page 3655

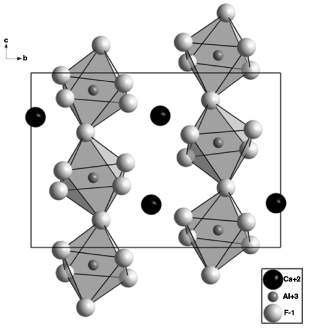

View of β-$CaAlF_5$, exhibiting isolated chains of AlF_6^{3-} octahedra sharing opposite corners.

Structural disorder in $Ba_{0.6}Sr_{0.4}Al_2O_4$

Koichiro Fukuda, Tomoyuki Iwata and Takashi Orito

Page 3662

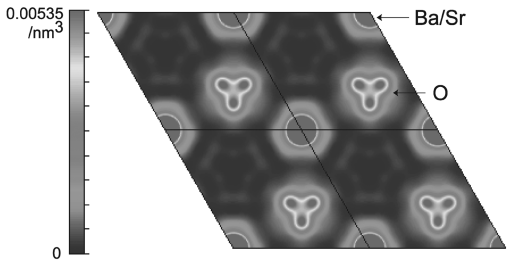

Two-dimensional electron density distribution map showing positional disorder of oxygen atoms in $Ba_{0.6}Sr_{0.4}Al_2O_4$.

Single-crystal synthesis and structure refinement of the $LiCoO_2$–$LiAlO_2$ solid-solution compounds: $LiAl_{0.32}Co_{0.68}O_2$ and $LiAl_{0.71}Co_{0.29}O_2$

Yasuhiko Takahashi, Norihito Kijima and Junji Akimoto

Page 3667

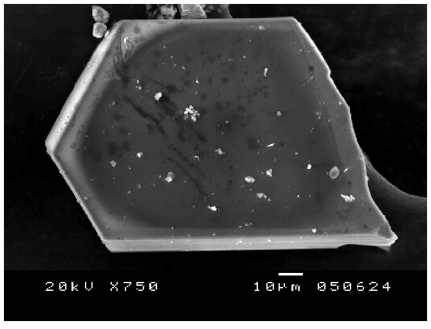

SEM photograph of a transparent $LiAl_{0.71}Co_{0.29}O_2$ single crystal.

Dehydrogenation kinetics of as-received and ball-milled $LiAlH_4$

A. Andreasen, T. Vegge and A.S. Pedersen

Page 3672

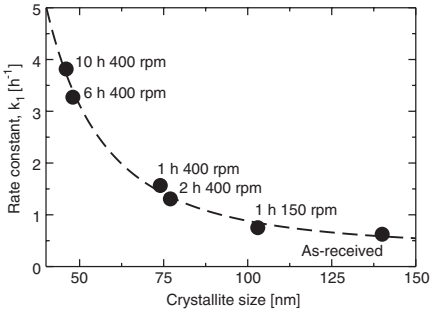

Effect of ball milling on kinetics. Rate constants for the dehydrogenation of lithium tetrahydroaluminate into trilithium hexahydroaluminate as a function of crystallite size obtained from XRPD line broadening.

Electronic behavior of three oxygen non-stoichiometric Fe^{4+}/Fe^{3+} oxoperovskites

H.D. Zhou and J.B. Goodenough

Page 3679

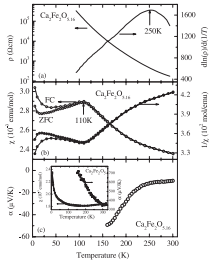

Temperature dependences of (a) resistivity $\rho(T)$ and $d(\ln \rho)/d(1/T)$; (b) molar magnetic susceptibility $\chi(T)$ and its inverse $1/\chi(T)$; and (c) thermoelectric power $\alpha(T)$ for $Ca_2Fe_2O_{5.16}$. Inset of (c): Temperature dependences of magnetic susceptibility $\chi(T)$ and thermoelectric power $\alpha(T)$ for $Ca_2Fe_2O_5$.

Synthesis and structural, spectroscopic and magnetic studies of two new polymorphs of $Mn(SeO_3)\cdot H_2O$

Aitor Larrañaga, José L. Mesa, José L. Pizarro, A. Peña, Roger Olazcuaga, María I. Arriortua and Teófilo Rojo

Page 3686

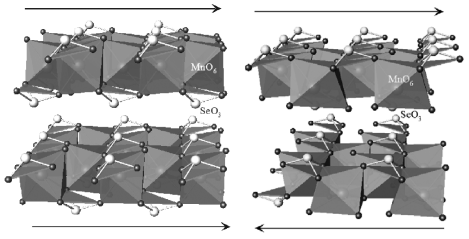

Crystal structures of two polymorphs of $Mn(SeO_3)\cdot H_2O$.

Continued

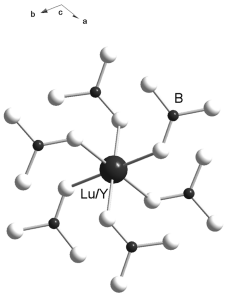

Even though these compounds, $YBa_3B_9O_{18}$, $LuBa_3(BO_3)_3$, α-$YBa_3(BO_3)_3$ and $LuBO_3$, have different atomic structures, they have the common structural feature of each yttrium or lutetium ion bonded to six separate BO_3 groups, i.e., octahedral $RE(BO_3)_6$ (RE = Lu or Y) moiety. This octahedral $RE(BO_3)_6$(R-E = Lu or Y) moiety seems to be an important structural element for efficient X-ray excited luminescence of those compounds, as are the edge-sharing octahedral TaO_6 chains for tantalate emission.

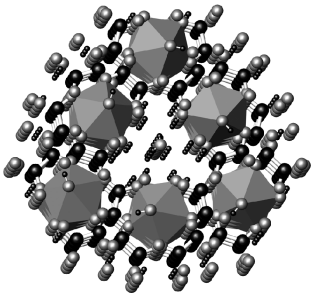

An open-framework three-dimensional indium oxalate $[In(OH)(C_2O_4)(H_2O)]_3 \cdot H_2O$ (**1**) was synthesized by hydrothermal reaction. Disordered water molecules are filled into the channels. It crystallizes in the trigonal system with space group $R3c$, $a = 18.668(3)$ Å, $c = 7.953(2)$ Å at 298 K.

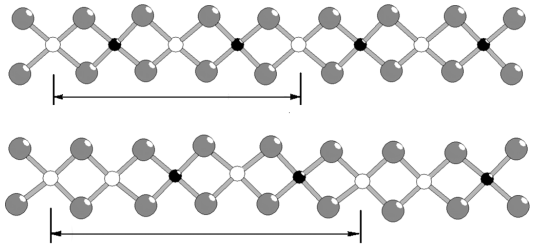

CuO_2 chains in $Na_3Cu_2O_4$ (above) and $Na_8Cu_5O_{10}$ (below).

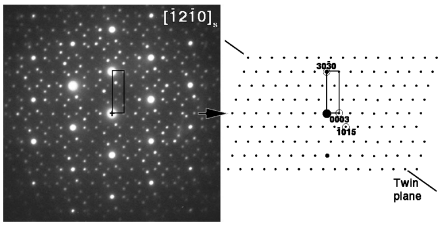

The scheme at the left of the $[\bar{1}\,2\,\bar{1}\,0]_s^*$ pattern shows one of the two twins present in the $[\bar{1}\,2\,\bar{1}\,0]_s^*$ pattern and the indexation of this twin.

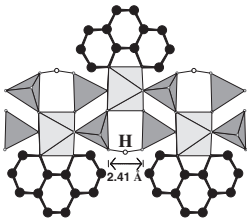

Two hydrothermally synthesized organic–inorganic hybrid compounds consist of 1-D chains of strictly alternating GaO_4N_2 octahedra and phosphate tetrahedra, which extend into 3-D supramolecular arrays via π–π stacking interactions of *phen* ligands and hydrogen bonds. ^2H MAS NMR spectroscopy was applied to study the very short hydrogen bonds.

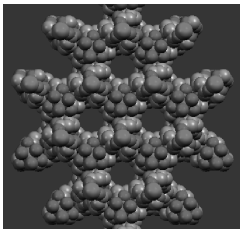

A reaction between Sm_2O_3, iminodiacetic acid (H_2Idad), CuO, and H_2O has allowed the synthesis of one nanoporous 3D open framework Cu(II)–Sm(III) coordination polymer, $[\{Sm_2Cu_3(Idad)_6\} \cdot 8H_2O]_n$ (**1**) and then magnetic behavior of the compound, $[\{Gd_2Cu_3(Idad)_6\} \cdot 8H_2O]_n$ (**2**), with a similar structure was studied.

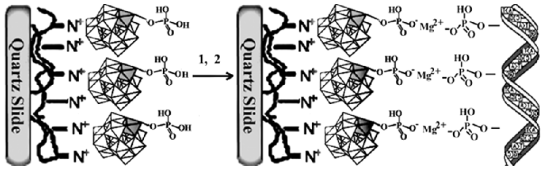

Key steps of immobilization of DNA to the {PDDA/$SiW_{11}Co–PO_4$} film, **1** $MgCl_2$ aqueous of 5 mM, **2** DNA aqueous.

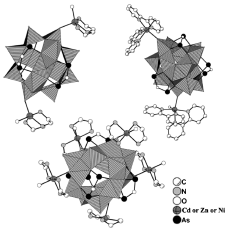

Three inorganic–organic hybrid solid materials based on $[As_8V_{14}O_{42}(H_2O)]^{4-}$ cluster building blocks bridging by transition metal complexes have been obtained by hydrothermal reaction and characterized by single-crystal X-ray diffraction. These compounds exhibit a wave-like chain, a tube-shaped chain and a rare two-dimensional structure containing interwinding puckery layers. Variable temperature susceptibility measurements demonstrate the presence of antiferromagnetic interaction between V^{IV} cations in two one-dimensional structures.